Title
COMPARISON OP BAUD STRUCTURES AND CHARGE DISTRIBUTIONS OF COPPER AND SILVER

Permalink
https://escholarship.org/uc/item/3b10n92h

Authors
Fong, C.Y.
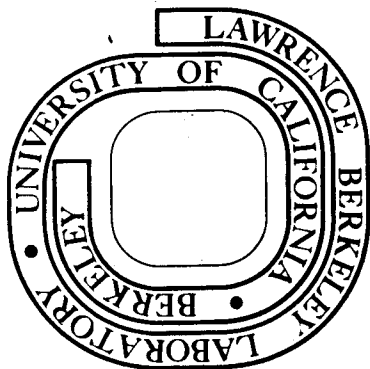Walter, J.P.
Cohen, Marvin L.

Publication Date
1974-11-01

COMPARISON OF BAND STRUCTURES AND CHARGE
DISTRIBUTIONS OF COPPER AND SILVER

C. Y. Fong, J. P. Walter, and Marvin L. Cohen

November, 1974

DISCLAIMER

0 0 0 0 0 0 2 0 0 0 0 0

COMPARISON OF BAND STRUCTURES AND

CHARGE DISTRIBUTIONS OF COPPER AND SILVER

C. Y. Fong[*]

Department of Physics, University of California
Davis, CA 95616

J. P. Walter[†] and Marvin L. Cohen[§]
Department of Physics, University of California

and

Inorganic Material Research Division
Lawrence Berkeley Laboratory, Berkeley, CA 94720

1

Abstract

.The band structures of copper and silver calculated using the empirical pseudopotential method are presented. The density of states for silver obtained from the band structure is compared with photo-emission experiments. The charge distributions of the two metals were calculated in the (100) plane. A comparison of the distributions is made with reference to the results of the band structures.

I. Introduction

The feasibility of obtaining good quality single crystals of noble metals has motivated many experimental studies on these crystals. Among these studies, optical and photoemission experiments have contributed significantly to our understanding of the electronic properties of these materials. Ehrenreich and Philipp[1] performed the first systematic measurements of the optical spectra for these metals with $0. \leqslant \hbar\omega \leqslant 24. eV$. To experimentally determine the origins of the structures in the spectrum of copper, Gerhardt[2] measured the change of the reflectivity by applying strains along different directions in the sample. Recently, the wave-length modulation technique has also been applied to optical studies of the noble metals[3,4]. As for the uv photoemission experiments, Berglund. and Spicer[5] have performed detailed studies on Cu and Ag. Later, Krolikowski and Spicer[6] have improved the measurements on Cu and Ag and extended their measurements to Au. More recently, Smith[7] used

2

the derivative technique to measure the energy distribution curves of the noble and transition metals. The energies of the structures in the spectra were accurately determined. The results obtained from both optical and photo-emission measurements provided information about the relative energies of the valence and conduction bands and the density of states of the valence bands.

The first complete band structure of a noble metal was calculated by Segall[8] for Cu using the Green's function method. Burdick[9] calculated the band structure of Cu by the argumented plane wave method (APW) with the potential originally obtained by Chodorow[10]. Band structures of both Cu and Ag were calculated by Snow[11] using the self-consistent APW method. The nonrelativistic and relativistic band structure of Ag has also been calculated by Christensen[12]. Most of these results have been compared to the results of photoemission data.

To understand the optical specta, Ehrenreich and Philipp[1] have used the band structure of Segall to make a qualitative identification of the structure in their spectra. Later, Mueller and Phillips[13] proposed a combined interpolation scheme of the pseudopotential method and the tight-binding method. The wavefunctions obtained from this method were used to calculate the dipole matrix elements. There were discrepancies between the theory and the experiment especially in the low energy region. Two of the present authors have added to the local pseudopotential method a $\ell=2$ nonlocal pseudopotential[14] to calculate the band structures of Cu and Ag by fitting to the photoemission data, and the optical gap of Cu determined by Gerhardt. We also used the actual wavefunctions instead of the pseudo wavefunctions to calculate the dipole moments. The results agree reasonably well with the experimental data and show that most of the structure in the optical spectra of noble

metals are still primarily due to one-electron processes. The same conclusion
was reached later by Williams, et al[15] using the Korringa-Kohn-Rostoker
method.

As we discussed above, most efforts on studies of the electronic
properties of Cu and Ag were concentrated on the optical properties
and the photoemission data. There are, however, some x-ray measurements
and calculations of form factors on Cu,[16,17] but there is a scarcity
of information about the bonding properties of these metals. Charge
density studies have been made on semiconductors[18], simple metals[19],
layer compounds[20] and transition metal compounds[21]. This paper re-
presents the first attempt for charge density calculations in noble
metals. Since the band structures of Cu and Ag obtained by the empirical
pseudopotential method (EPM) agree reasonably with the optical and photo-
emission data, the pseudo wavefunctions except the ones relating to
s and p bands near the atomic site, can be considered to be reasonably
accurate for calculating the charge distributions of these metals. It
is hoped that these calculations will stimulate experimental investigations
in this area. We present here the charge densities of Cu, Ag and make
comparisons between the two metals using the calculated band structures.
The band structure of Ag calculated by the empirical pseudopotential method
has not been given elsewhere. We shall discuss the band structure of the
two metals with emphasis on the results of Ag in Section II. In Section III,
the charge distribution of 6 individual bands and the total densities of the
occupied states will be presented. A comparison between the distribution of
these two noble metals will be made also.

II. Band Structures of Silver and Copper

The band structure of Ag along different symmetry lines is plotted in Fig. 1. The optical spectrum of Ag calculated from this band structure shows a difference of 0.22eV from experiment in the position of the minimum for $R'(\omega)/R(\omega)$[4]. This difference was attributed to the fact that we have fitted the pseudopotential to the photoemission data. The density of states obtained from this band structure is shown in Fig. 2. There are structures at -4.2,-5.0,-5.2,-5.8,-6.3 and -6.7eV with respect to E_F, the Fermi energy. The structures reported by Smith[7] in his photoemission measurements are -4.1, -4.9, -5.6, -6.2 and -6.9eV. The agreement between the theory and the experiment is of the order of 0.2eV. The weak structure at -5.0eV in the calculation is sensitive to the potential, whereas the other structures are insensitive to the potential. A comparison of a few important energy gaps with some representative first principle calculations and the origin of the structure in the density of states are given in Tables I and II repectively.

Since our purpose is to compare the charge distributions of Ag and Cu obtained from the results of the band structure calculations, we include our previously reported band structure of Cu[14] in Fig. 3. A comparison of the pseudopotentials for these two noble metals is given in Table III. There are several important differences in the two band structures. (a) The energy between the top of the d-bands to E_F is 1.66eV in Cu and 3.82eV in Ag. The d-bands in Ag are farther away from E_F than in the case of Cu. (b) The s-p gap ($\Gamma_1 \rightarrow X_4'$) is 11.8eV in Cu and is 8.5eV in Ag. (c) Because of the differences in (a) and (b), the d-band overlap with the s-like band in Ag. It is especially clear in the Δ direction, where

Δ_1 and Δ_2' cross each other. This causes the X_3 band to be lower than X_1 and Γ_1. Therefore, the lowest band in Ag has more d-like character whereas in Cu it is primarily a hybridized band of s and d states.

III. Charge Distributions of Copper and Silver

To calculate the charge distributions of the two noble metals, we have set up a mesh using 46 points in 1/48th of the Brillouin zone. The wavefunctions are first obtained by diagonalizing the pseudopotential Hamiltonian at the $\vec{k}$-points which are the center of the cube defined by the mesh. Then the 47 other wavefunctions were generated by the symmetry operators pertinent to the crystal. The total charge is normalized to two electrons/band-primitive cell.

In Figs. 4a to 9b, we have plotted the charge distributions of the individual bands which are either completely or partially occupied. The "a"'s refer to Cu while the "b"'s refer to Ag. All these sections are in the (100) plane. The edges are in the units of their respective lattice constants. The atoms are at the corners and at the center of the plane. In these plots, the most significant differences are exhibited in Figs. 4A, 4b and 5a, 5b. The four lobes (contours with the values close to 5.5 in Fig. 4a) around the atom in Fig. 4a point along the axes of the cubic cell. These lobes are due to the hybridization of the d-states (X_1, K_1, L_1^{ℓ}) to the s-like states (Γ_1). The shapes of the contours resemble the ones in Fig. 5b. In Fig. 5a, the distributions are for the pure d-like states (Δ_2', X_3, Σ_3, Λ_3). The lobes are pointing along the face diagonal. Comparing this with the results of Ag, the contours are much like the

ones in Fig. 4b. This is due to the fact that the X_3 and X_1 bands of
Ag are reversed in order and the crossing of Δ_1 and Δ_2' happens very
near Γ_1, as we discussed in Section III. Therefore, the lowest energy
band of Ag has predominantly d-like character. The strong hybridization
of the d-states to s-states is also manifested in the magnitude of the
distributions. If the hybridization is of the same extent in both
metals, one expects the maximum of the contours for Ag to be smaller
than the ones for Cu because the volume of the primitive cell for Ag
is bigger than the volume of Cu. In Figs. 4a and 5b, the slightly
large maximum value of the contours of Ag indicate that there is more
mixing of the d-states. The rest of the distributions are quite similar
in shape for both cases. The lobes of the d-states rotate back and forth
by 45° as the band indices increase, so that the d-states experience
the maximum attractive potential from the nucleus, and the crystals will
be in the lowest energy state. Figs. 9a and 9b show the distributions
of the partially occupied d-p hybridized bands (6th band in Figs. 1 and
3). The distribution of Ag is rather uniform compared with all lower
energy bands and the corresponding case of Cu. This means there are
more d-like states in the 6th band of Cu than that is in Ag. The larger
differences in the separation of the d-band with respect to E_F of Ag causes
the distribution to be more like the case of simple metals[19].

The total charge densities are about 14% less than what they should be,
because we have used a coarse mesh as discussed in the beginning of this
section. Since we are interested in the qualitative features of the
charge density of the two noble metals, this error is not significant
and the main features of the distributions should be correct. However,

if a calculation of the x-ray form factors is made to compare with the x-ray data, a finer mesh is definitely needed.

The total charge distributions of the occupied states are shown in Figs. 10a and 10b. The maximum of the contours associated with each atom occurs near 1/4 -th of the interatomic distance. These are made up primarily from the lobes of the d-states. The contours exhibit nearly perfect spherically symmetric shape around the atom. Slight deviations happen in the regions midway between the atoms. It is just what one would expect: The completely filled d-states and an additional s-like electron is expected to give the calculated spherical distribution for the total charge density. This also explains why the APW method using the muffin-tin potential works so well for the noble metals.

The charge distributions of the unoccupied portion of the 6th conduction band are shown in Figs. 11a and b. The shapes of the contours and the directions which the lobes are pointing are the same for Cu and Ag. As we see in Figs. 1 and 3, the angular momentum character is the same for these bands for the two metals. The magnitudes of the contours in Figs. 11a and b are also comparable. The conduction bands of the two metals as suggested here are quite similar. As we mentioned earlier, the charge distributions of these s-p states, within a radius of 1/10-th of the side of the square around the atoms are not expected to be accurate, because the pseudo wavefunctions are used in the calculations.

In summary, we have presented the band structure of Ag calculated by the EPM and compared it with the one of Cu. The density of states derived from the band structure of Ag gives reasonable agreement to the photo-emission data. The electronic charge distributions for Cu and Ag have been calculated in the (100) plane using the pseudo wavefunctions from

the band structures. The effect of the crossover of the X_1 and X_3 bands in Ag is manifested in the charge distributions of the individual bands. Furthermore, because the d-bands in Ag are about 4.eV below E_F, whereas in Cu, the separation is about 2.eV, the charge distributions show clearly that there is a stronger mixing of the d-states with the s-state in the lower energy bands and a smaller hybridization effect for the 6th band in Ag. Except for the distributions of the second and the third bands in Cu, the lobes of the d-states rotate 45° back amd forth as the band indices change in order to have the strongest possible attractive potential for the d-states. The features of the distributions of the d-states should be more accurately represented than the ones of the s and p states near the atomic site because the detailed nature of the d-states has been taken into account by the $\ell = 2$ nonlocal pseudopotential.

Acknowledgment

References

1. H. Ehrenreich and H. R. Philipp, Phys. Rev. 128, 1622 (1962).

2. U. Gerhardt, Phys. Rev. 172, 651 (1968).

3. C. Y. Fong, M. L. Cohen, R. R. L. Zucca, J. Stokes and Y. R. Shen, Phys. Rev. Letters 25, 1486 (1970).

4. J. Stokes, Y. R. Shen, Y. W. Tsand, M. L. Cohen and C. Y. Fong, Phys. Letters 38, 347 (1972).

5. C. N. Berglund and W. E. Spicer, Phys. Rev. 136,A 1030 (1964).

6. W. F. Krolikowski and W. E. Spicer, Phys. Rev. 185, 882 (1969); ibid B1, 478 (1970).

7. N. W. Smith, Phys. Rev. B3, 1862 (1970); ibid B9 1365 (1974).

9

References

8. B. Segall, Phys. Rev. $\underline{125}$, 109 (1962).

9. G. A. Burdick, Phys. Rev. $\underline{129}$, 138 (1963).

10. M. Chodorow , Phys. Rev. $\underline{55}$, 675 (1939).

11. E. C. Snow, Phys. Rev. $\underline{171}$,785 (1968); ibid $\underline{172}$, 708 (1968).

12. N. E. Christensen, Phys. Status Solidi, $\underline{54}$, 551(1972).

13. F. M. Mueller and J. C. Phillips, Phys. Rev. $\underline{157}$, 600 (1967).

14. C. Y. Fong and M. L. Cohen, Phys. Rev. Letters, $\underline{24}$, 306 (1970).

15. A. R. Williams, J. F. Janak and V. L. Morizzi, Phys. Rev. Letters $\underline{28}$, 671 (1972).

16. R. J. Temkin, V. E. Henrich and P. M. Raccah, Phys. Rev. B$\underline{6}$, 3572 (1972).

17. F. J. Arlinghaus, Phys. Rev. $\underline{153}$, 743 (1967).

18. M. L. Cohen, Science $\underline{179}$, 1189 (1973); and references there in.

19. J. P. Walter, C. Y. Fong and M. L. Cohen, Solid State Comm. $\underline{12}$, 3031 (1973).

20. C. Y. Fong and M. L. Cohen, Phys. Rev. Letters, $\underline{32}$, 720 (1974).

21. D. J. Chadi and M. L. Cohen, Phys. Rev. B$\underline{10}$, 496 (1974).

10

Table Captions

Table I.   A comparison of a few important energy gaps for the present

results on Ag with representative first principle

calculations.

Table II.   Identifications of the structure in the density of states of

Ag.

Table III.   Pseudopotential parameters of Cu and Ag.

Figure Captions

Figure 1.   Band structure of Ag.

Figure 2.   The density of states of Ag.

Figure 3.   Band structure of Cu.

Figure 4a.   Charge distribution of band 1 for Cu in (100) plane.

Figure 4b.   Charge distribution of band 1 for Ag in (100) plane.

Figure 5a.   Charge distribution of band 2 for Cu in (100) plane.

Figure 5b.   Charge distribution of band 2 for Ag in (100) plane.

Figure 6a.   Charge distribution of band 3 for Cu in (100) plane.

Figure 6b.   Charge distribution of band 3 for Ag in (100) plane.

Figure 7a.   Charge distribution of band 4 for Cu in (100) plane.

Figure 7b.   Charge distribution of band 4 for Ag in (100) plane.

Figure 8a.   Charge distribution of band 5 for Cu in (100) plane.

Figure 8b.   Charge distribution of band 5 for Ag in (100) plane.

Figure 9a.   Charge distribution of band 6 (occupied portion) for Cu in (100)
plane.

Figure 9b.   Charge distribution of band 6 (occupied portion) for Ag in (100)
plane.

Figure Captions

TABLE I

energy gaps	Snow[11] Self-Consistent APW 5/6 Slater $\rho^{1/3}$	Christensen[*] APW 2/3 Slater $\rho^{1/3}$	Ballinger[**] and Marshall (Green's function)	Present results
s-d				
$\Gamma_1 \rightarrow \Gamma_{25}'$	1.22 eV	3.24 eV	1.63 eV	0.58
$\Gamma_1 \rightarrow \Gamma_{12}$	2.08	4.34	2.86	1.74
$\Gamma_1 \rightarrow X_1$	-0.19	1.21	0.07	-0.45
$\Gamma_1 \rightarrow X_3$	-0.05	1.59	0.14	-0.56
$\Gamma_1 \rightarrow X_2$	2.76	5.17	3.67	2.7
$\Gamma_1 \rightarrow X_5$	3.01	5.36	3.94	2.96
$\Gamma_1 \rightarrow L_1^{\ell}$	0.08	1.51	0.41	-0.17
$\Gamma_1 \rightarrow L_3^{\ell}$	1.18	3.17	1.77	0.58
$\Gamma_1 \rightarrow L_3^{u}$	2.82	5.52	3.67	2.69
s-p				
$\Gamma_1 \rightarrow X_4'$	9.07	9.15	9.38	8.50
$\Gamma_1 \rightarrow L_2'$	6.85	6.80	7.34	6.34
$L_2' \rightarrow E_F$	0.095	0.76	0.34	0.44
$L_2' \rightarrow L_1^{u}$	—	5.33	4.08	4.17

* N. E. Christensen, Phys. Status Solidi 31, 635 (1969).

** R. A. Ballinger and C. A. W. Marshall, J. of Phys. C: Solid State Physics 2, 1822 (1969).

13

TABLE II

Present Calculations	Photoemission Measurement	Identifications
-4.2	-4.1	X_2, L_3^u and K_2
-5.0 ⎫	-4.9	$\begin{cases} \Gamma_{12} \\ \Delta_1^u \end{cases}$
-5.2 ⎭		
-5.8	-5.6	Volume effect of 3rd and 4th bands.
-6.3	-6.2	$\Gamma_{25}{}'$, Σ_3, Σ_1
-6.7	-6.9	L_1^ℓ, K_1

* u and ℓ means upper and lower bands.

TABLE III

Pseudopotential Parameters	Copper	Silver
$V^*(\|\bar{G}\|^2 = 3)$	0.0131 Ryd.	0.022 Ryd.
$V(4)$	0.0189	0.023
$V(8)$	0.0162	0.0362
$V(11)$	0.0014	0.0162
A_2	-9.9044	-8.4610
R_M	0.814 Å	0.9447 Å
α	0.433	0.43
K	$2.63(2\pi/a)$	$2.08(2\pi/a)$
a	3.615 Å	4.08 Å

* Defined in reference 14.

Fig. 1

-14-

Fig. 2

Fig. 3

Fig. 4a

0.5

5

2

BAND I

Fig. 4b

BAND 2

Fig. 5a

0.5

6.5   5

BAND 2

Fig. 5b

BAND 3

Fig. 6a

BAND 3

Fig. 6b

BAND 4

Fig. 7a

-24-

BAND 4

Fig. 7b

BAND 5

Fig. 8a

BAND 5

Fig.8b

BAND 6
(BELOW E_F)

Fig. 9a

BAND 6
(BELOW E$_F$)

Fig. 9b

TOTAL
VALENCE
BANDS

Fig. 10a

4

16

28
28

16

4

TOTAL
VALENCE
BANDS

Fig. 10b

BAND 6
(ABOVE E_F)

Fig. 11a

BAND 6
(ABOVE E$_F$)

0.75

1.5

1.75

Fig. 11b